Blucher Mechanical Engineering Proceedings
May 2014, vol. 1 , num. 1
www.proceedings.blucher.com.br/evento/10wccm

NEAR FIELD STRUCTURE OF TWIN TANDEM INCLINED AND VARIABLY ELEVATED JETS IN CROSSFLOW

A. Radhouane[1] , N. Mahjoub[2], H. Mhiri[1], G. LePalec[3], P. Bournot[3]

[1] Unit of Heat Transfer and Thermodynamics of the Industrial Processes, Department of Energtics, National Engineering School of Monastir, route of Ouardanine, 5000 Monastir, Tunisia (radhouane_amina@yahoo.fr)

[2] Preparatory Institute to Engineering Studies of Monastir, 5000 Monastir, Tunisia

[3] IUSTI, UMR CNRS 6595, Technopôle Château-Gombert, 5 rue Enrico Fermi, 13013 Marseille, Cedex 20, France

Abstract. *Jets in crossflow are of a high interest since they are central to a variety of industrial applications like fuel injectors, smokestacks, cooling of turbine blades and dilution holes in gas turbine combustors. The present work aims at performing an extensive exploration of the field generated by double tandem jets interacting with an oncoming crossflow.*
The jets are inclined (60°) and variably but similarly elevated as discharged from nozzles whose height varied between 0 and 5 cm. The jet nozzles discharge a characteristic industrial fume under a temperature gradient of 100 K with reference to the surrounding atmosphere temperature.
Consideration is given to a steady, three-dimensional, incompressible and turbulent flow. The resolution of the different conservation law equations is carried out by means of the Computational Fluid Dynamics (CFD) software, Fluent, together with the Reynolds Stress Model and a non uniform grid system.
Once validation towards previous experimental data reached, emphasis was particularly given to the induced interactions, namely jet-to jet, jets-to-crossflow and jets-to-jet nozzles interactions. Description was carried out in terms of the developed vortical structures, the established streamlines and further dynamic features, under an injection ratio R equal to 2.
Examination was given to the symmetry plane and to different streamwise cross-sections. Such a consideration illustrated decreasing deviation and downstream reattachment of increasingly high jets. This issue is of particular interest as deeply involved in pollutants' dispersion in urban zones. Its resolution may provide viable solutions for reducing and/or preventing from inhabitants' contamination.

Keywords: *twin jets, crossflow, jet elevation, near field, vortical structures.*

1. INTRODUCTION

The structure of the flowfield resulting from the interaction of twin jets in crossflow, also called transverse jets, is of high interest due to its being central to a variety of industrial applications. Fuel injectors, smokestacks, cooling of turbine blades and electronic devices, dilution holes in gas turbine combustors, etc. are some of these applications.

The importance of jets in crossflow configuration comes also from its dependence in several parameters. The variation of the involved parameters may affect significantly the resulting flowfield, and induce severe environmental damages, mainly consisting of atmospheric and water pollution.

Establishing a consistent examination of the generated flowfield is then likely to reveal the most determinant mechanisms governing its progression, as well as the favorable conditions to enhance it. Taken into account, these considerations may prevent from expected problems in preconception phases and provide viable solutions for already built models, of course accordingly to the applications' target.

Jets' elevation, arrangement and separation distance, jets to crossflow velocity ratio (injection ratio), jets to crossflow temperature gradient, etc. are some of these affecting parameters. We propose to dedicate the present work to the impact of jets' elevation on the flowfield they induce while interacting with an oncoming crossflow, under a temperature gradient, in an inline configuration.

To our knowledge, the unique paper having introduced the question in the literature, in an inline arrangement is that of Radhouane et al. [1], where it was question of two similar inline inclined jets in crossflow. The jet nozzles were placed three diameters apart, and discharged a non reactive fume at a variable elevation under a given injection ratio ($R = 2$). The paper mainly explored the fume progression by examining the distribution of the pollutants' mass fraction along different longitudinal positions. Jets' elevation proved to promote the obstacle like flow developed and trapped between the increasingly high jet nozzles.

Further papers dedicated to inline double jets in crossflow are available in the literature. However flush-mounted and elevated jet cases were considered separately without being compared. This is the case in papers of Briggs [2,3], Anfossi et al. [4] and Gangoiti et al. [5].

Based upon Briggs' two semi-empirical models [2.3], relative to two inline similarly elevated jets, Anfossi et al. [4] developed a "virtual" stack concept able to compute the rise of the resulting plume of two inline variably elevated jets. The model was first validated in the case of stacks of similar height and emission conditions with reference to Brigg's experimental data [2]. The model was then upgraded to cover stacks of different elevations and validated with reference to experimental data. The model was finally corrected, in terms of ground level concentrations, with reference to the empirical expression of Montgomery et al. [6] together with Briggs' models [2, 3].

Twin elevated inline jets in crossflow were also explored by Gangoiti et al. [5] in the context of numerical simulations within real atmospheric situations (wind shear and stability variations with height) and water phase changes. For the matter, jets containing a mixture of four components, namely dry combustion gas, dry air, water vapor and liquid water, were discharged within an oncoming crossflow, under complex meteorological conditions. Laminar

and turbulent atmospheres were included by using the parameterization by Netterville [7], suited to a wind sheared atmosphere rather than to flat wind profiles. As to plume trajectories, they were described in terms of plume merger in a multiple source, condensation and re-evaporation, rise in turbulent winds, rise in light winds and in stratified atmosphere with wind shear. Observations made over these data and more particularly plume trajectories and final rise were compared to the numerical model predictions and a set of classical formulations used for regulatory models whose mismatching was mainly due to the presence of complexities not allowed for in that formulation.

Further works compared both elevated and flush-mounted jets in crossflow, though at a side by side arrangement. That was the case of Bunsierst et al. [8] who considered twin jets, placed two diameters apart, outside the crossflow boundary layer, in a subsonic wind tunnel and under an injection ratio equivalent to $R = 3.3$ and a Reynolds number of $Re = 6200$. Results, consisting of turbulent velocity and momentum data, were compared in both cases. Diffuse interactions take place between the jet wakes and the stacks' wakes in the near field of elevated jets, and intense interactions develop within the jet wakes, indicating significant contributions of the jets' vortices to the counter-rotating vortex pair (CVP) downstream.

Comparisons of the behavior of elevated and flush mounted jets in crossflow are more abundant in the single jet case. Moore [9] is pioneer in the domain since he first handled the question in the early seventies. His work consisted of correlating the trajectory of a plume of hot gas from a power station by means of the plume rise above the source, the rate of heat emission, wind speed at 1.5 stack heights and downwind distance. This correlation was suited to different geometries (stack heights), meteorological conditions (neutral, unstable atmospheres) and showed to be dependent on initial conditions (efflux velocities) and plume characteristics (density).

The plume trajectory of a jet discharged from a stack variably high was also explored by Netterville [7] together with the transition to the leveling phase and the leveling itself in a turbulent atmosphere. Leveling-off is actually induced by ambient turbulence in a non-stable atmosphere with constant wind speed and vertical air temperature gradient. It was modeled for a plume from a talk stack by assuming a loss of effective mass by detrainment of plume material into the environment through the action of eddies. Leveling is modeled either apart from the rising trajectory, after an abrupt transition from the buoyancy dominated phase to the atmosphere, or by fitting a curve to experimental data.

Flush-mounted and elevated single jets in crossflow were also discussed by Karagozian [10] in the context of a review paper that provided a background on this type of jet models, their applications, detailed features and controlling mechanisms. Particular emphasis was put on physical phenomena that dominate the dynamics, mixing, breakup, and/or reactive processes associated with the canonical jet injected into uniform crossflow. Such explorations are likely to bring light on complex stability characteristics and provide efficient control solutions.

We can see then that variably elevated jets in crossflow are not very well documented in the literature, and even less in the case of twin inline jets in crossflow. Single jet explorations were slightly more discussed; while comparison of elevated and flush-mounted jets were scarcer. Based upon these observations, we intend to provide in the present work an exclusive

exploration of double, inline, inclined and variably high jets in crossflow, including both high and flush-mounted jet models.

Our interest will be particularly focused on the generated near field since it shields diverse and complex interactions, namely jet-jet, jet-nozzle, jet-crossflow and jet-ground interactions. We propose to track these interactions in terms of the induced vortical structures and of the corresponding dynamic features.

2. PRESENTAION OF THE PROBLEM

The inline arrangement of twin jets in crossflow is geometrically very simple in spite of the jets' initial inclination toward the mainstream direction. Nevertheless, the flowfield resulting from their interaction is highly complex due to the double interaction between both jets on one hand and between the jets and the oncoming crossflow on the other hand. This complexity is further emphasized by the variation of the governing parameters. In the present work, attention will be devoted to jets' elevation impact, and the first step to reach this goal is to realize a consistent modeling of the configuration.

Figure 1 presents the limit cases: the one on the left corresponds to the flush-mounted jets ($h = 0\ cm$) while the one on the right presents the most elevated case ($h = 5\ cm$). Dimensions, orientation and velocity scales, etc. are derived from former experiments that served for the validation of the model. The corresponding data were tracked by means of the Particle Image Velocimetry (PIV), whose set-up, different phases and all related details were deeply described in reference [11].

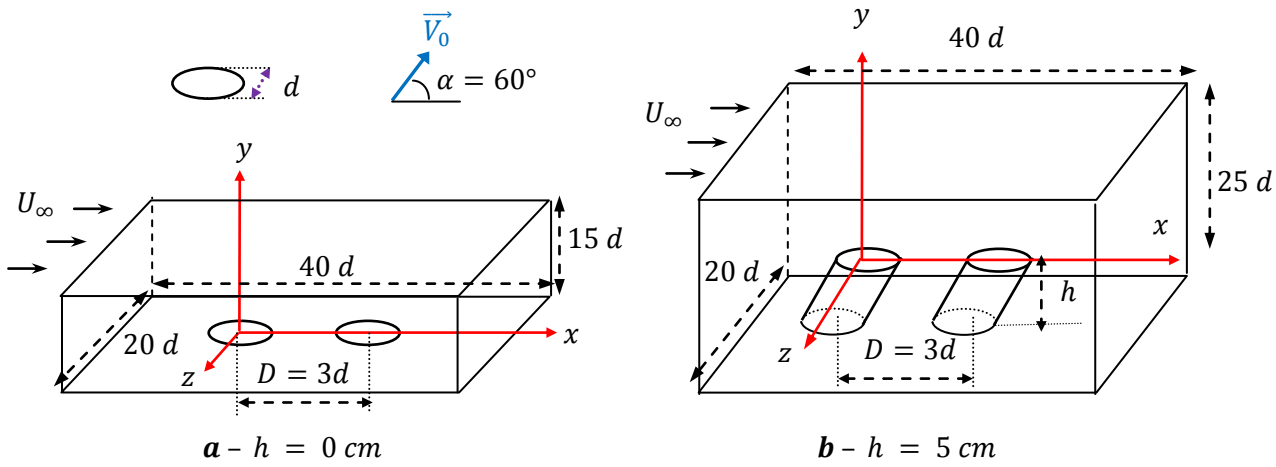

a – $h = 0\ cm$ ***b*** – $h = 5\ cm$

Figure 1. Considered configurations:
(a) flush-mounted ($h = 0\ cm$) jet model, (b) most elevated jet model ($h = 5\ cm$)

The reproduced geometry consists of twin inline jet nozzles placed apart at a constant distance of three diameters ($D = 3d$). The emitting nozzles are cylinders that were inclined according to an angle of $\alpha = 60°$ and razed at different levels from the injection ground. This procedure resulted in an elliptic shape of the exit cross-sections as shown in fig. 1, characterized by a small (d) and a large ($d/\sin\alpha$) diameter, respectively in the streamwise (z) and longitudinal directions (x).

A Cartesian coordinate system is adopted to scale the different reigning fields. This choice is motivated by the asymmetry of the resulting flowfield in spite of the symmetry of the handled geometry, as observed by Smith et al. [12] and verified by Radhouane et al. [11]

3. COMPUTATIONAL SET-UP

Numerically, consideration is given to a steady, three-dimensional, incompressible and turbulent flow. The different conservation law equations, the Navier Stokes equations, describing the resulting flowfield interactions, are discretized and then written in a Cartesian coordinate system, centered within the exit section of the rear jet nozzle:

$$\frac{\partial}{\partial x_i}(\bar{\rho}\widetilde{u_\iota}) = 0 \tag{1}$$

$$\frac{\partial}{\partial x_j}(\bar{\rho}\widetilde{u_\iota}\widetilde{u_j}) = -\frac{\partial \bar{p}}{\partial x_i} + \frac{\partial}{\partial x_j}\left(\mu\frac{\partial \widetilde{u_\iota}}{\partial x_j} - \overline{\rho u_i^{"} u_j^{"}}\right) + (\overline{\rho_\infty} - \overline{\rho})g\delta_{ij} \tag{2}$$

$$-\rho\overline{u_i^{"}u_j^{"}} = \mu_t\left(\frac{\partial \widetilde{u_\iota}}{\partial x_j} + \frac{\partial \widetilde{u_j}}{\partial x_i} - \frac{2}{3}\delta_{ij}\frac{\partial \widetilde{u_k}}{\partial x_k}\right) - \frac{2}{3}\bar{\rho}k\delta_{ij} \tag{3}$$

with

$$\frac{\partial}{\partial x_j}(\bar{\rho}\widetilde{u_j}\tilde{T}) = \frac{\partial}{\partial x_j}\left[\left(\frac{\mu}{Pr} + \frac{\mu_t}{\sigma_t}\right)\frac{\partial \tilde{T}}{\partial x_j}\right] \tag{4}$$

$$\frac{\partial}{\partial x_j}(\bar{\rho}\widetilde{u_j}\tilde{f}) = \frac{\partial}{\partial x_j}\left[\left(\frac{\mu}{Sc} + \frac{\mu_t}{\sigma_f}\right)\frac{\partial \tilde{f}}{\partial x_j}\right] \tag{5}$$

To fully characterize the fluctuating functions and variables developing in a similar complex three dimensional flow, we introduced the Reynolds Stress Model (RSM). The RSM is a second order turbulent closure model that uses the dissipation rate of the turbulent kinetic energy in order to compute the destruction of turbulence. It contains more information about the turbulent forces than the simpler approaches and includes their anisotropy by taking separately into account the production and history of each Reynolds stress term. Its efficiency to better describe this kind of configurations has already been demonstrated in a previous paper [14].

The introduction of the RSM model leads to the resolution of the following equation:

$$\underbrace{\frac{\partial}{\partial x_k}\left(\bar{\rho}\widetilde{u_k}\overline{u_i^{"}u_j^{"}}\right)}_{C_{ij}} = \underbrace{\frac{\partial}{\partial x_k}\mu\frac{\partial}{\partial x_k}\left(\overline{u_i^{"}u_j^{"}}\right)}_{D_{ij}^L} - \bar{\rho}\underbrace{\left[\overline{u_i^{"}u_k^{"}}\frac{\partial \widetilde{u_j}}{\partial x_k} + \overline{u_j^{"}u_k^{"}}\frac{\partial \widetilde{u_i}}{\partial x_k}\right]}_{P_{ij}} + D_{ij}^T + G_{ij} + \emptyset_{ij} + \varepsilon_{ij} \tag{5}$$

with

$$D_{ij}^T = -\frac{\partial}{\partial x_k}\left[\bar{\rho}\overline{u_i^{"}u_j^{"}u_k^{"}} + \overline{P'(\delta_{kj}u_i^{"} + \delta_{ik}u_j^{"})}\right] \tag{6}$$

$$G_{ij} = -\overline{\rho}\beta\left[g_i\overline{u_j^{"}T^{"}} + g_j\overline{u_i^{"}T^{"}}\right] \tag{7}$$

$$\emptyset_{ij} = \overline{P'\left(\frac{\partial u_i^{"}}{\partial x_j} + \frac{\partial u_j^{"}}{\partial x_i}\right)} \tag{8}$$

$$\varepsilon_{ij} = -2\mu \overline{\frac{\partial u_i^{"}}{\partial x_k}\frac{\partial u_j^{"}}{\partial x_k}} \tag{9}$$

where $C_{ij,}$ D_{ij}^{L}, P_{ij}, D_{ij}^{T}, G_{ij}, ϕ_{ij}, ε_{ij}, *are* respectively, the convective term, the molecular diffusion, the stress production, the turbulent diffusion, the buoyancy production, the pressure strain and the dissipation rate of the turbulent kinetic energy [11].

The equations of the turbulent kinetic energy (k) and of the dissipation rate of the kinetic energy (ε) associated with the second-order model are defined as follows:

$$\frac{\partial}{\partial x_i}(\bar{\rho}\tilde{u}_i k) = \frac{\partial}{\partial x_j}\left[\left(\mu + \frac{\mu_t}{\sigma_k}\right)\frac{\partial k}{\partial x_j}\right] + \frac{1}{2}(P_{ii} + G_{ii}) - \overline{\rho\varepsilon} \tag{6}$$

$$\frac{\partial}{\partial x_i}(\bar{\rho}\tilde{u}_i \varepsilon) = \frac{\partial}{\partial x_j}\left[\left(\mu + \frac{\mu_t}{\sigma_\varepsilon}\right)\frac{\partial \varepsilon}{\partial x_j}\right]\frac{C_{\varepsilon 1}}{2}\frac{\varepsilon}{k}(P_{ii} + C_{\varepsilon 3}G_{ii}) - C_{\varepsilon 2}\bar{\rho}\frac{\varepsilon^2}{k} \tag{7}$$

with

$$P_{ii} = 2\mu_t\left(\frac{\partial \tilde{u}_i}{\partial x_i}\right)^2 \tag{8}$$

$$G_{ii} = 2\beta g_i \frac{\mu_t}{\sigma_t}\frac{\partial \tilde{T}}{\partial x_i} \tag{9}$$

$$\mu_t = C_\mu \bar{\rho}\frac{k^2}{\varepsilon} \tag{10}$$

For more information concerning the constants introduced in the different equations see reference [14].

Standard discretization was carried out on the pressure term while the momentum, the turbulence kinetic energy, the turbulence dissipation rate, the different Reynolds stresses and the temperature were discretized by means of the first order upwind scheme. We remind that the different conservation laws were solved by means of the finite volume method. Corrections were brought on the pressure and velocity calculations by means of the Patankar and Spalding's algorithm "SIMPLE" [15]. The convergence of the calculations was obtained when the sum of the normalized residues reached 10^{-3}.

A non-uniform grid system was adopted and particularly tightened in the near field of the discharging nozzles to describe well the mechanisms shielded in this zone. The mesh system corresponding to each model was adopted after an elaborate study of the mesh sensibility. Herein, we have to mention that no low-Reynolds number model was adopted near to the wall, as in this region Reynolds number is based upon the uniform velocity of the mainstream and the hydraulic diameter.

Before varying the injection height, validation was carried out in the basic case of air flush-mounted jets ($h = 0$) discharging in air crossflow under no temperature variation ($\Delta T = 0$) and under an injection ratio equivalent to $R = 1.29$.

Once validated [11], the model was upgraded to fit better the reality by considering a temperature difference equivalent to $\Delta T = 100\ K$ between the emitted jets and the oncoming crossflow. The jets discharged under an injection ratio equivalent to $R = 2$, contained a char-

acteristic industrial fume, whose composition is specified in tab. 1, even though it was assumed to be non reactive for simplification sakes.

These data together with the different adopted boundary conditions are summarized in the table 1.

Table 1. Adopted boundaries conditions

Boundaries	Velocity	Temperature	Mass fraction	Kinetic energy	Dissipation rate
Nozzle sections	$\tilde{u} = V_0 \cos\alpha$ $\tilde{v} = V_0 \sin\alpha$ $\tilde{w} = 0$	$\tilde{T} = T_0 = 403.15$	$\tilde{f} = f_0$	$k = k_0 = 10^{-3} V_0^2$ [16]	$\varepsilon = \varepsilon_0 = \frac{k_0^{3/2}}{0.5d}$ [16]
Crossflow	$\tilde{u} = U_0$ $\tilde{v} = \tilde{w} = 0$	$\tilde{T} = T_\infty = 303.15\ K$	$\tilde{f} = f_\infty$	$k = 0$	$\varepsilon = 0$
Walls	$\tilde{u} = \tilde{v} = \tilde{w} = 0$	$\frac{\partial \tilde{T}}{\partial y} = 0$	$\frac{\partial \tilde{f}}{\partial y} = 0$	$\frac{\partial k}{\partial y} = 0$	$\frac{\partial \varepsilon}{\partial y} = 0$
Remaining boundaries	$\frac{\partial \tilde{u}}{\partial n} = \frac{\partial \tilde{v}}{\partial n} = \frac{\partial \tilde{w}}{\partial n} = 0$	$\frac{\partial \tilde{T}}{\partial n} = 0$	$\frac{\partial \tilde{f}}{\partial n} = 0$	$\frac{\partial k}{\partial n} = 0$	$\frac{\partial \varepsilon}{\partial n} = 0$
Fume composition	N_2: 76.9%, CO_2: 20.9%, O_2: 1.8%, SO_2: 0.4%				

Finally, the following nozzle heights were tested, namely $h = 0, 1, 2, 3$ and $5\ cm$. As shown in figure 1. Accordingly, progressively higher domains were considered relatively to the progressively higher injection levels. The other dimensions (width and length) were tested and proved not to interfere in the flow structures.

4. DISCUSSION:

Once discharged and independently from the level of their discharge level with reference to the domain ground, the jets are bound to interact with the surrounding crossflow, with each other and with the surrounding walls. The occurrence and order of these interactions depend on the initial conditions such as the injection ratio, the inclination of the injection nozzles, the jets' spacing etc.

In our case, a jet spacing of three diameters was adopted together with an injection ratio equivalent to $R = 2$. The latter, superior to one, is simply considered to detect better the progression of the jets as it supposes a stronger jet velocity and then a more pronounced progression within the environing domain. The initial inclination ($\alpha = 60°$) helps enhancing the jets' progression as it enlarges the interaction zone (longitudinally)as observed and deeply explained and demonstrated by Radhouane et al. [11, 17].

We come now to the impact of the level of the injection cross-section. It is first discussed in figure 2 over the progression of each of the jets' central core trajectories.

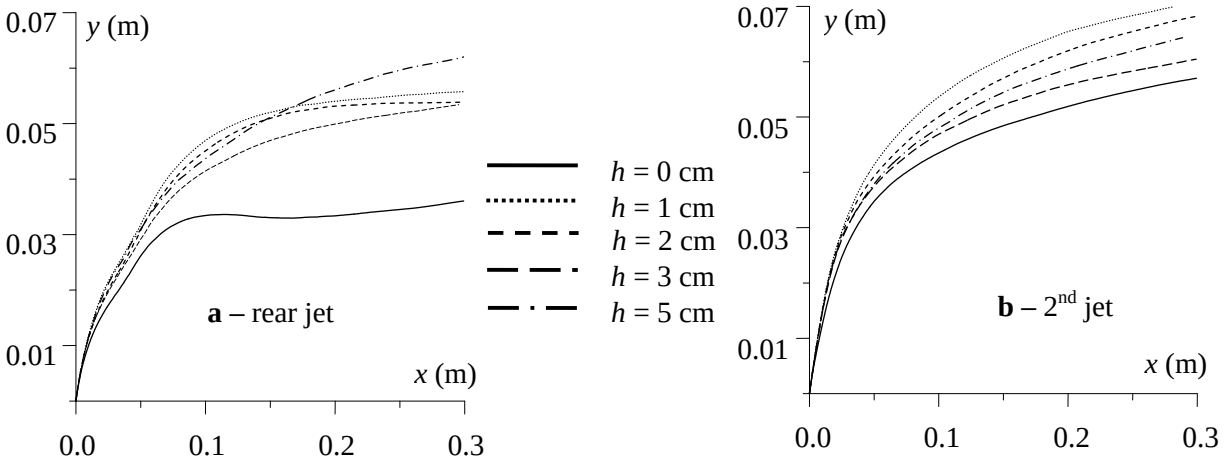

Figure 2. Impact of jets' elevation over the proper progression of each of the jets: **a**) Rear jet, **b**) downstream jet

Jets' elevation effect over the downstream jet trajectory is more regular and better established than the one relative to the rear jet. We mainly see that the transition between flush-mounted and elevated cases brings a consistent jet rise (fig. 2-b). The jet is actually "liberated" from the ground wake, promoting its vertical expansion within the domain. Carrying on elevating the injection level leads to the reverse effect since the jet trajectory is lowered for the following elevation cases ($h = 1, 2$ and $3\ cm$), which reveals a limited effect of the jets' elevation.

The sudden increase in the jet rise is due to the vanishing of the wake effect. In fact, once liberated from the ground wake, the jet is free from the corresponding reattachment effect that used to retain its plume. The higher the jet is discharged, the less its plume is enlarged, justifying the progressively lower jet trajectory.

The highest case, $h = 5\ cm$, shows a further inversion of the trajectory trend (fig. 2-b) as it rises once again. This may be related to the rear jet behavior. The later precisely has a much more complicated trend due to its critical location. In fact, its prior location implies a direct and consistent confrontation with the oncoming crossflow. Varying the injection level would only bring further complication on the generated flow, and that's we see on the rear jet trajectory: a consistent and more pronounced jet rise is reached due to the canceled reattachment effect. Discharging the first jet at a higher level, similarly to the following one, decreased its rise even though the trajectories are not as distinct in this location due to the crossflow's more pronounced effect interference. Finally, when the jet is discharged at the highest injection level, it reaches the highest rise at the far field (fig. 2-a). Reaching the second jet location at such a consistent rise together with the crossflow may be at the origin of the collapse of the downstream jet's trajectory.

Figure 3 reports a closer consideration of both jets' trajectories under each of the elevation cases. It presents the distribution of streamlines issuing from the central core of both jet nozzles. We clearly see the more significant deflection of the rear jet independently of its emission height due to its prior location, and then its direct interaction with the surrounding flow. The rear jet plays the role of an obstacle that "protects" the following one from a consistent deflection, enabling it to diffuse more significantly within the oncoming crossflow.

The gap between both jets' progression however decreases when they are sent at a higher level from the ground. The rear jet is always undergoing the crossflow's deflection effect; however this mechanism is significantly lightened when the first jet gets free from the ground's reattachment. At the highest injection case (fig. 3-e), we assist even at quasi-similar jets' trajectories.

Herein, we would like to point out the shifting of both x and y axes. This is simply due to the assumption we've done in the beginning, stating that the origin of the Cartesian coordinate system is placed at the center of the rear jet exit section. This section is progressively higher due to the injection nozzles elongation and farther in the longitudinal direction due to the nozzles' inclination.

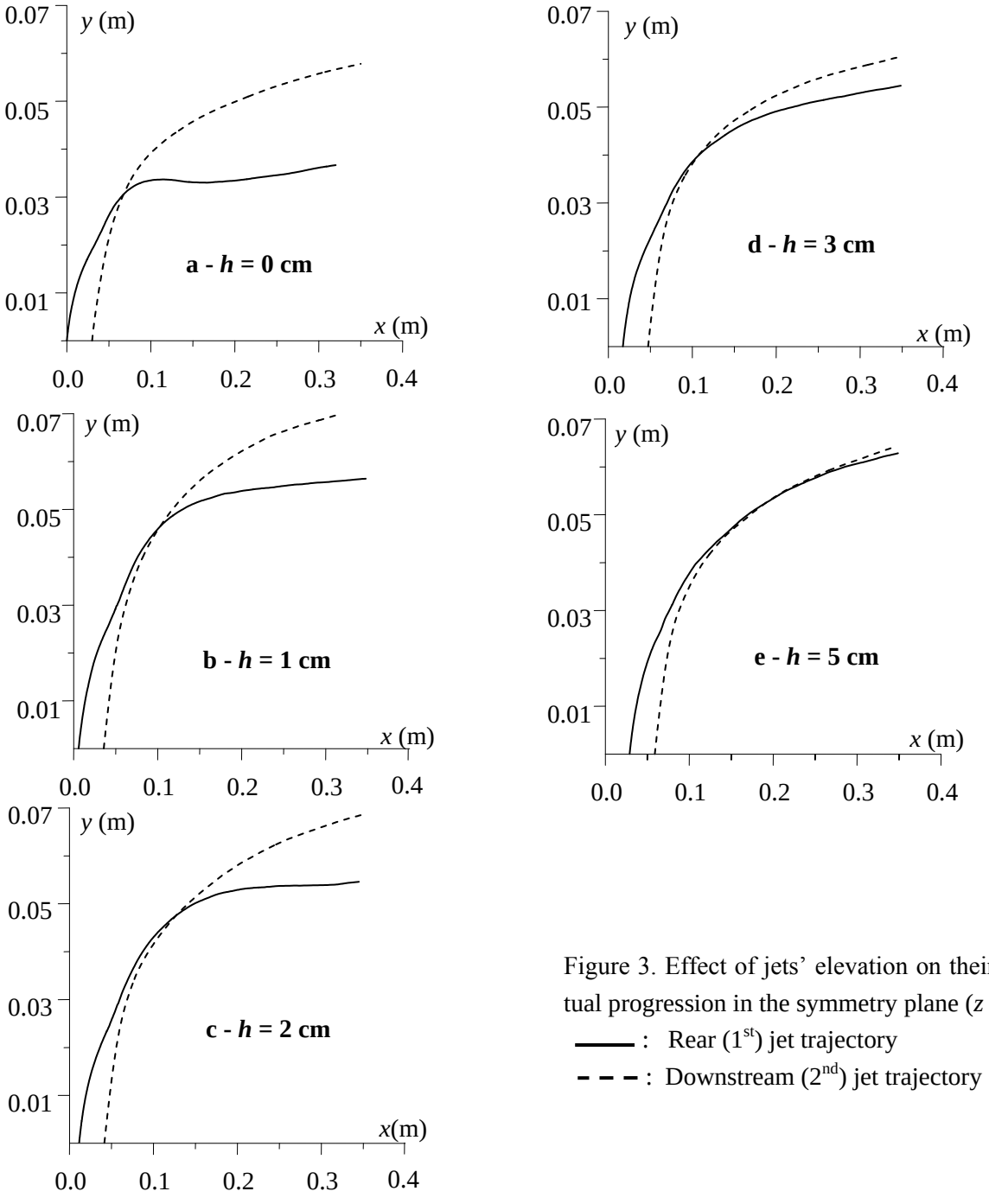

Figure 3. Effect of jets' elevation on their mutual progression in the symmetry plane ($z = 0$):
——— : Rear (1st) jet trajectory
– – – : Downstream (2nd) jet trajectory

The impact of the jets' elevation is further detailed in fig. 4 where we present the progression of the temperature field in the symmetry plane ($z = 0$). Structurally, we see progressive detachment of the jet plumes as soon as they are sent farther from injection plate.

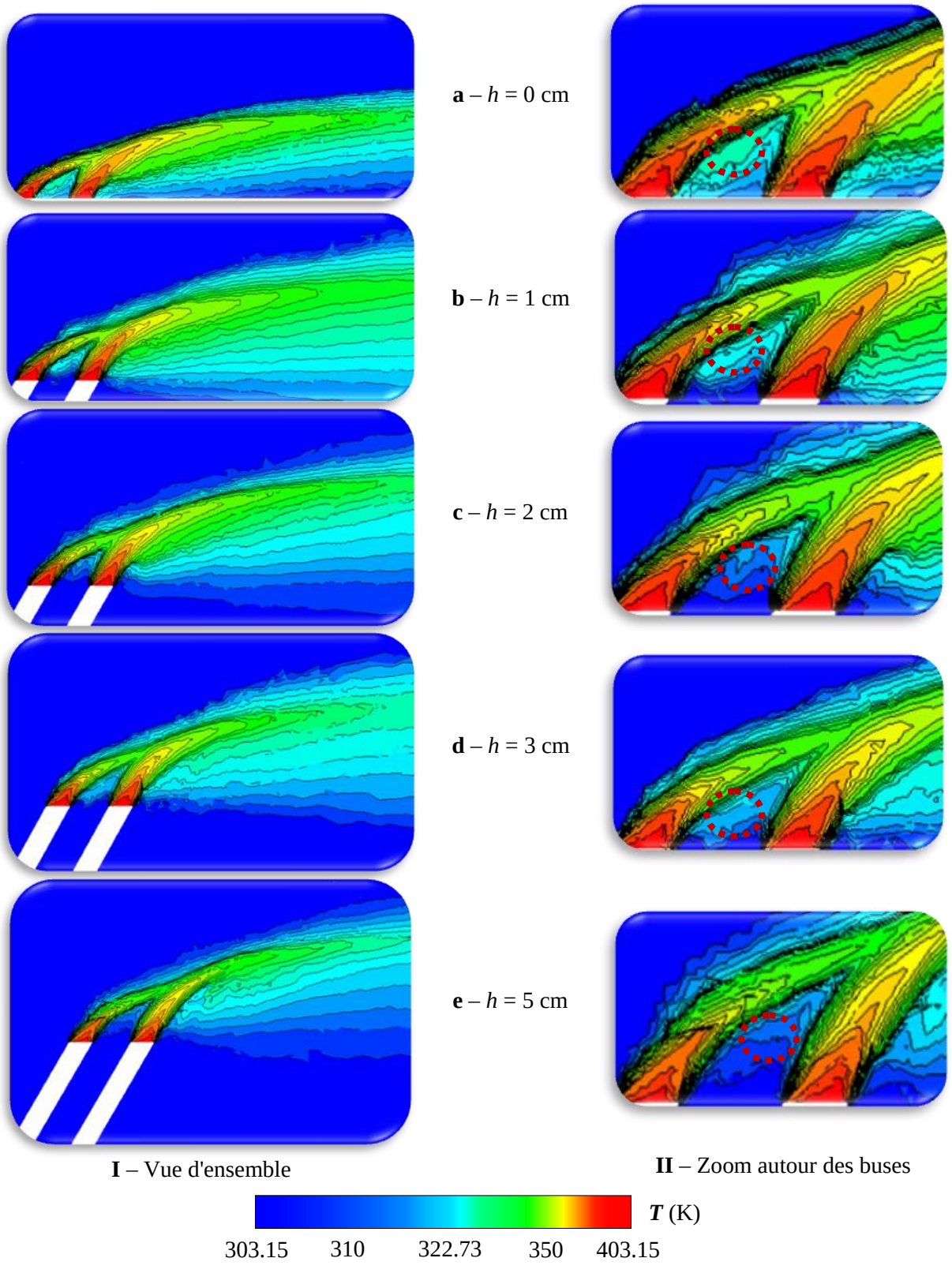

Figure 4. Effect of jets' elevation on the induced thermal field developed in the symmetry plane ($z = 0$)

The reattachment concerns the in-between jet nozzles as well as the downstream region, and the fig. 4 stresses particularly on the trapped zone that was highlighted in the zoomed view (fig. 4-II). When the jets are sent flush to the ground, and in presence of the both the crossflow and the initial inclination, the jets are deflected consistently and deflected against the injection plate. The consistent deflection is at the origin of the complex flowfield induced in the in-between jet zone, it is characterized by a temperature change illustrated by the variation in the temperature iso-contours (the encircled zone in fig. 4-II-a).

When the jets are sent higher from the injection plate, the thermal field established in this zone is progressively less affected as the temperature accuses less consistent variations, illustrated by the quasi-unchanged iso-contours of the temperature. Figure 5 emphasizes on these observations and generalizes them as it expands them laterally. In fact, temperature contours are plotted in fig. 5, at the level of the injection exit section ($y = h$), under the most determinant injection cases: flush-mounted jet case ($h = 0\ cm$), the highest injection case ($h = 5\ cm$) and an intermediate case ($h = 2\ cm$).

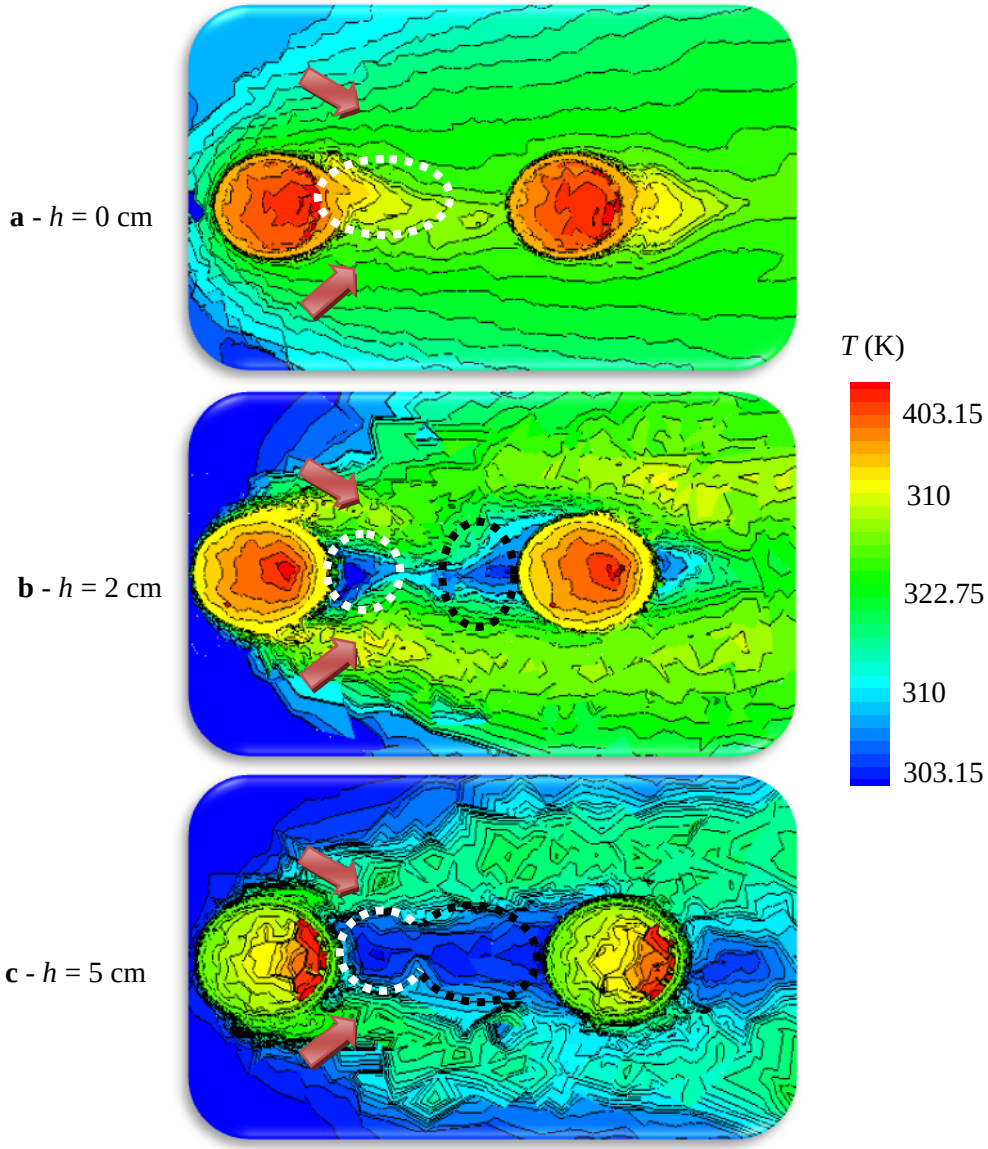

Figure 5. Effect of jets' elevation on temperature distribution in the near field (0<x<5d) developed at the level of the injection cross-section ($y = h$)

The weakened variation of the in-between nozzles' zone is well apparent here through the development of a progressively unchanged thermal field. A similar character is also apparent downstream of the second jet nozzle. This is mainly due to the further vertical expansion of the highly emitted jets, and then their decreasing lateral interference with the surrounding flow.

The second prominent feature to discuss in the same figure is the asymmetry of the developed resulting flowfield. This flow character is apparent under all cases but is much more emphasized under the highest injection case (fig. 5-c). The asymmetry concerns the deviation of the trapped flow in the in-between nozzles' zone (encircled) as well as the global shape of the horseshoe peripheral structures (indicated with arrows).

5. CONCLUSION

The present study was dedicated to the exploration of the flowfield resulting from the interaction of twin inline, inclined, elliptic, non reactive and variably high fume jets with an oncoming cooler uniform air crossflow. This exploration was carried out by means of the finite volume method together with the second order RSM (Reynolds Stress Model) turbulent closure model and a non uniform grid system.

Consideration was given to the development of the streamlines issuing from the central core of each of the discharging jet nozzles. It was mainly shown that the rear jet accuses a much more consistent deflection which promotes its reattachment to the ground. Sending the jets at a higher level reduces this effect on both jets, promoting their global rise within the surrounding flow, and leading to the establishment of stagnant flow at the level of the ground.

Contours of the thermal field, taken at the symmetry plane as well as at the discharging cross-section levels, comfort these observations and expand them as they reveal the asymmetric character of the resulting flowfield. The asymmetry is even reinforced with the injection height.

Effects of the injection height are to be further explored over the resulting flowfield in terms of velocity, vortical structures and mass transfer. We could even further explored this configuration under the variation of further affecting parameters such as the jet nozzles' interspace, arrangement or exit-section shape, etc.

6. NOMENCLATURE

Symbol	Description	Unit
C_p	Specific heat	J/(kg K)
D	Nozzles' spacing	m
G_k	Term of production due to buoyancy forces	kg/(m s^3)
P_k	Term of production due to the mean gradients	kg/(m s^3)
R	Velocity ratio	No unit
S_{ij}	Mean strain rate	No unit
T	Temperature	K
U_∞	Crossflow velocity	m/s
V_0	Injection velocity	m/s
d	Jet nozzle diameter	m
f	Mass fraction	No unit
g	Gravitational acceleration	m/s^2
h	Jet nozzle height	

k	Kinetic energy of turbulence	m^2/s^2	μ	Kinetic viscosity	kg/(m s)
$\overline{u_i'' u_j''}$	Reynolds stress	m^2/s^2	μ_t	Turbulent (or eddy) viscosity	kg/(m s)
u_i, u_j	Velocity components along the i and j directions		ν	kinematic viscosity	m^2/s
u, v, w	Velocity components along x, y, and z directions	m/s	ρ	Density	Kg/m^3
x, y, z	Cartesian coordinates	m		**Subscripts**	
			∞	Crossflow conditions	No unit
	Greek Symbols		0	Jet exit section	No unit
α	Injection Angle with reference to the free stream (x axis)	°		**Superscripts**	
β	Thermal expansion coefficient	K^{-1}	$\bar{}$	Reynolds average	No unit
δ_{ij}	Kronecker symbol (=1 if i=j and 0 if i≠j)	No Unit	$\tilde{}$	Favre average	No unit
ε	Dissipation rate of the Turbulent kinetic energy	No unit		**Dimensionless groups**	
κ	Thermal diffusivity	m^2/s	Pr	Prandtl number ($Pr = \mu Cp/\lambda$)	No unit
λ	thermal conductivity,	W/(mK)	Re	Reynolds number ($Re = u_i\, d/\nu$)	No unit
			Sc	Schmidt number ($Sc = \nu/\kappa$)	No unit

7. REFERENCES

[1] Radhouane, A., Mahjoub Saïd, N., Mhiri, H., Le Palec, G., Bournot, P., "Dispersion of twin inclined fume jets of a variable height within a crossflow", *Defect and Diffusion Forum*, vols. 312-315, pp.929-934, 2011.

[2] Briggs, G.A., "Plume rise from multiple sources ", *Proceedings of cooling tower environmen*t held at University of Maryland, pp. 161-179, 1974.

[3] Briggs, G.A., "Plume Rise Predictions. Lectures on Air Pollution and Environmental Impact Analyses". *American Meterological Society*, pp. 59–111, 1975.

[4] Anfossi, D., Bonino, G., Bossa, F., Richiardone, R., "Plume rise from multiple sources: a new model", *Atmospheric Environment*, 12, pp.1821-1826, 1978.

[5] Gangoiti, G., Sancho, J., Ibarra, G., Alonso, L., Garcïa, J.A., Navazo, M., Durana, N., Ilardia, J.L., "Rise of moist plumes from tall stacks in turbulent and stratified atmospheres", *Atmospheric Environment* 31(2), pp. 253-269, 1997.

[6] Montgomery, T.L., Norris W.B, Thomas F.W., Carpenter S.B., "A simplified technique used to evaluate atmospheric dispersion of emissions from large plants". *J. Air. Poll. Control Ass*. 23, pp. 388-457, 1973.

[7] Netterville D.D.J., "Plume rise, entrainment and dispersion in turbulent winds". *Atmospheric Environment*, 24A, pp. 1061-1081, 1990.

[8] Bunsirisert, K., Orrala, C., Rahai, H.R, "Profiles of two elevated side-by-side turbulent jets in a crossflow", *43rd AIAA Aerospace Sciences Meeting and Exhibit*, Reno, Nevada, 2005.

[9] Moore, D.J., "A comparison of the trajectories of rising buoyant plumes with theoretical/empirical models, *Atmospheric Environment*, 8, pp. 441-457, 1974.

[10] Karagozian, A.R., "Transverse jets and their control", *Progress in Energy and Combus-*

tion Science, pp.1-23., 2010.

[11] Radhouane, A., Mahjoub Saïd, N., Mhiri, H., Le Palec, G., Bournot P., "Impact of the initial streamwise inclination of a double jet emitted within a cool crossflow on its temperature field and pollutants dispersion", *Heat and Mass Transfer*, Springer, 45(6), pp. 805-823, 2009.

[12] Smith, S.H., Mungal M.G., "Mixing, structure and scaling of the jet in crossflow". *J. Fluid Mech* 357:83–122,1998

[13] Radhouane, A., Mahjoub Saïd, N., Mhiri, H., Le Palec, G., Bournot, P., "Impact of the Temperature of Twin Inclined Tandem Jets on their Dynamic Interaction with a Cooler Oncoming Crossflow", *Proceedings of the 7th International ASME Conference on Nanochannels, Microchannels and Minichannels* (ICNMM2009-82029), 22-24 June, Pohang, South Korea, 2009

[14] Mahjoub Said N., Mhiri, H., Golli, S., Le Palec, G., Bournot, P., "Three dimensional numerical calculations of a jet in an external crossflow: application to pollutant dispersion", ASME *J. of heat transfer*, 125, 2009.

[15] Patankar, S.V., Spalding, D.B., "A calculation procedure for heat, mass and momentum transfer in three-dimensional parabolic flows", *Int. J. Heat Mass Transf*., 15, pp. 1787–1806, 1972.

[16] Demuren, A.O., Rodi, W., "Three Dimensional Numerical Calculations of Flow and Plume Spreading Past Cooling Towers", *J. Heat Transfer*, 109, pp. 113–119, 1987.

[17] Radhouane, A., Bournot, H., Mahjoub Saïd, N., Mhiri, H., Le Palec, G., "Numerical and experimental study of a double jet inclination variation on its dynamic evolution within a crossflow", *Heat and Mass Transfer Journal*, 45(12), pp. 1597-1616, 2009.